J. Cent. South Univ. (2015) 22: 3698−3704
DOI: 10.1007/s11771-015-2912-0

Springer

Mechanical responses, texture and microstructural evolution of high purity aluminum deformed by equal channel angular pressing

WANG Bing-feng(汪冰峰)[1, 2, 3], SUN Jie-ying(孙杰英)[1], ZOU Jin-dian(邹金佃)[1], VINCENT Sherman[2], LI Juan(李娟)[1]

1. School of Materials Science and Engineering, Central South University, Changsha 410083, China;
2. Departments of Mechanical and Aerospace Engineering and Nanoengineering, University of California, San Diego CA 92093−0411, USA;
3. Key Lab of Nonferrous Materials of Ministry of Education (Central South University), Changsha 410083, China

Abstract: Ultrafine-grained (UFG) high purity aluminum exhibits a variety of attractive mechanical properties and special deformation behavior. Equal channel angular pressing (ECAP) process can be used to easily and effectively refine metals. The microstructure and microtexture evolutions and grain boundary characteristics of the high purity aluminum (99.998%) processed by ECAP at room temperature are investigated by means of TEM and EBSD. The results indicate that the shear deformation resistance increases with repeated EACP passes, and equiaxed grains with an average size of 0.9 μm in diameter are formed after five passes. Although the orientations distribution of grains tends to evolve toward random orientations, and microtextures (80°, 35°, 0°), (40°, 75°, 45°) and (0°, 85°, 45°) peak in the sample after five passes. The grain boundaries in UFG aluminum are high-angle geometrically necessary boundaries. It is suggested that the continuous dynamic recrystallization is responsible for the formation of ultrafine grains in high purity aluminum. Microstructure evolution in the high purity aluminum during ECAP is proposed.

Key words: equal channel angular processing (ECAP); aluminum; grain refinement; microstructure; mechanical property

1 Introduction

Ultrafine-grained (UFG) aluminum and its alloys exhibit a variety of attractive mechanical properties such as high strength combined with sufficient ductility, enhanced impact toughness, and super plasticity at high strain rates and low temperature [1]. UFG microstructures are the subject of extensive research efforts worldwide. Recently, special attention has been paid to various UFG metallic materials with traditional compositions processed by severe plastic deformation (SPD) process, such as equal channel angular pressing (ECAP) [2−6], high-pressure torsion (HPT) [7−8], multi-axial compression (MAC) [9−10] and accumulative roll-bonding (ARB) [11−13]. Of the various SPD processes available, ECAP is attractive because the simplicity of the process and tooling makes it cost effective and easy to perform.

Transmission electron microscopy (TEM) observations have been extensively employed to investigate the microstructure evolution during ECAP process. Depending on the materials and the processing method, various mechanisms have been proposed for the evolution of UFGs microstructure during ECAP. One of the mechanisms of UFGs evolution during ECAP is continuous dynamic recrystallization (cDRX), explained by IWAHASHI et al [14]. In their work, the initial massive reduction in grain size was achieved in the first passage through the die because the original grains break up into bands of subgrains; further pressings cause these sub-boundaries to evolve into high-angle grain boundaries. SALEM et al [15] compared the grains sizes of the commercial (99%) purity aluminum with the higher purity (99.998%) aluminum after consecutive pressing, and suggested that the discontinuous static recrystallization (dSRX) dominates in aluminum during pressing. For metals with low stacking fault energy, grain refinement in the Cu−Al alloys during ECAP was considered to operate by grain subdivision through twin fragmentations [16]. Strain-induced phase transformation during large plastic deformation also contributes to grain refinement. XU et al [17] and LIN et al [18] found that grain fragmentation takes place after ECAP as a result of the stress-induced phase transformation. However, the limited area illuminated in post-mortem TEM thinned

Foundation item: Project(12JJ2028) supported by the Hunan Provincial Natural Science Foundation of China; Project(201308430093) supported by the China Scholarship Council; Projects(201012200006, 2013zzts185, 2012zzts066) supported by the Freedom Explore Program of Central South University, China
Received date: 2014−09−22; **Accepted date:** 2015−01−31
Corresponding author: WANG Bing-feng, Associate Professor, PhD; Tel/Fax: +86−731−88876244; E-mail: wangbingfeng@csu.edu.cn

disks provides poor statistical information. Texture and grain boundary evolution play important roles in the understanding of metals deformation, especially in UFG materials. In order to characterize the microtexture evolution and grain boundary within the deformation section, electron backscatter diffraction (EBSD) is employed to examine the details of deformed samples. Compared to TEM, EBSD enables the observation of larger areas to obtain more statistically significant data on crystal orientations, boundary misorientations, etc. Therefore, the EBSD technique helps to elucidate the microstructure evolution and the grain boundary characteristics in metals during ECAP process, and understand the grain refinement mechanism in UFG materials.

The aims of this work are to obtain the mechanical responses of the high purity aluminum during ECAP process, characterize the microstructure and microtexture evolutions and grain boundary of the high purity aluminum during ECAP process, and discuss the grain refinement mechanism for UFG-Al.

2 Experimental

The material for this work is a high purity aluminum (about 99.998%) produced by ingot metallurgy. Cylindrical samples with 7 mm in diameter and 70 mm in height were machined from cylindrical ingots. The initial microstructure of the high purity aluminum is shown in Fig. 1, and the grain size is about 1.18 mm.

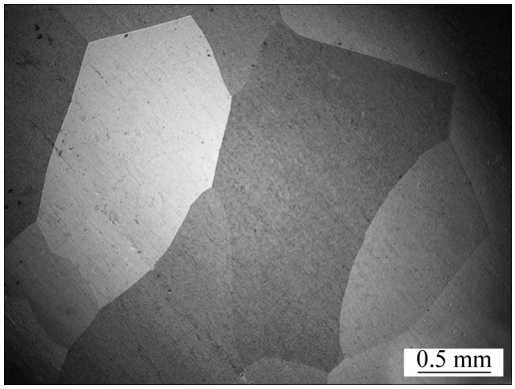

Fig. 1 Initial microstructure of high purity aluminum

For SPD of the samples, an ECAP die with two equal cross-section channels (7 mm in diameter) was used. The angle between two inner channels was 120° while the outer corner angle was 20°. Ram speed was 5 mm/min and the process was carried out at room temperature. In order to reduce friction, MoS_2 was used as a lubricant. CHANG et al [19] found that there was essentially no changes in the average grain size and aspect ratio when the process increased from 4 to 8 passes. Thus, the samples were subjected to five ECAP passes. An effective strain of 0.64 per pass was estimated [20]. Several specimens were pressed consecutively to avoid any difficulties in removing samples from the die, and the sample did not rotate between passes (route A).

Following ECAP, the small samples with a thickness of 0.5 mm were cut from the center of the extruded specimens, perpendicular to the extruding direction. The samples were reduced to a thickness of 0.10 mm using sandpaper, and then the foils were perforated by electropolishing in solution of 30% nitric acid and 70% methanol at 243 K. TEM observations were carried out with a Tecnai G^2 F20 transmission electron microscope operated at 200 kV. The grain size was defined as the average of the long and short axes of a grain. A high-resolution Helios Nanolab 600i scanning electro microscope (Opal, Oxford Instrument) operated at 20 kV was used to characterize the microtextures and grain boundaries within the electro-polished specimens. Different scanning step sizes were employed in different samples to vary the grain sizes. Due to limits imposed by angular resolution, only boundaries with misorientation greater than 1° were detected. EBSD data were analyzed using commercially available TSL-OIM software. From EBSD data, grain and sub-grain size, shape and misorientation were determined. White and black lines represent low (misorientation between 1° and 15°) and high (misorientation higher than 15°) angle grain boundaries, respectively.

3 Results and discussion

3.1 Mechanical responses of samples during ECAP processes

During the ECAP process, the stress and the pressing displacement of the first pass to the third pass are recorded in Fig. 2. The stress increases with the pressing displacement before the inflection point, and then the stress decreases. The values of the inflection points and the pressing displacements before the inflection points reveal the shear deformation resistance of the metal and the start of severe plastic deformation, respectively. It is can be seen that the inflection points increase from 320 MPa to 361 MPa, while the corresponding pressing displacements decrease gradually with the number of passes (Fig. 2). Therefore, the shear deformation resistances of the metal increase with the EACP passes.

3.2 Deformation microstructure in multi-pass pressing

The TEM images of the high purity aluminum after pressings are shown in Fig. 3. The sample after one pressing is comprised of cell structures elongated along the shear direction, and the grain size is significantly

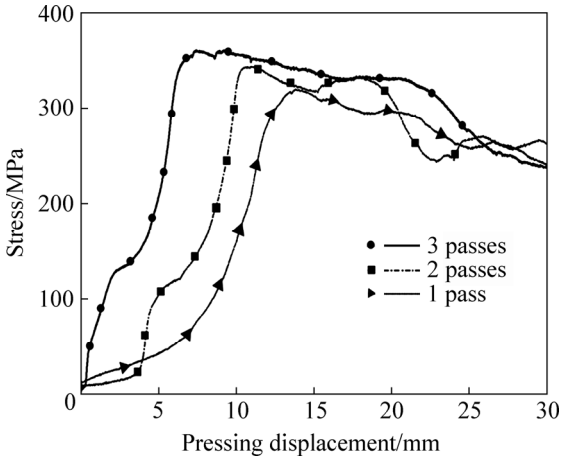

Fig. 2 High purity aluminum extrusion curves with different ECAP passes

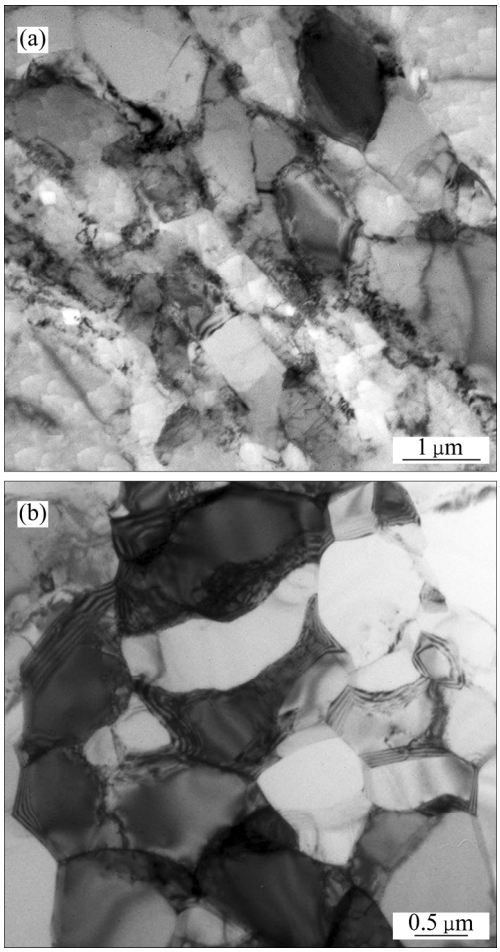

Fig. 3 TEM micrographs showing microstructure of high purity aluminum after ECAP: (a) First pass; (b) Fifth pass

reduced from an initiate grain size of about 1.18 mm to about 1.5 μm (Fig. 3(a)). After five passes of ECAP (an effective strain value of about 3.2), equiaxed grains of size of about 0.9 μm in diameter, well defined boundaries, and low dislocation density are formed (Fig. 3(b)). The grains in the sample after five ECAP passes are clearly refined and have a typical recrystallization character.

3.3 Microtexture measurement of samples

An orientation imaging micrograph (OIM) image of the initial high purity aluminum is shown in Fig. 4(a). The grain colors are determined by the orientation of each grain as depicted in the unit triangle. In this OIM image, as well as the following OIM images, the grain boundaries with misorientations higher than 15° (high angle boundaries, HABs) are shown as black lines, and the low angle boundaries (LABs) are marked by white lines. It can be seen that the microstructure of the initial materials consists of bulky grains separated by high angle boundaries. After the first pass of ECAP, regular arrays of elongated cells or subgrains are parallel to each other, and large band structures with similar color can be seen in the sample (Fig. 4(b)). This indicates that the subgrains have similar orientation. Figure 4(c) shows that the grains are refined and have distinctive structures with various orientations in a sample pressed five times. Therefore, the gradual appearances of colors which represent the misorientations of grains become more apparent with increased pressings.

From the measured orientations, the orientation distribution functions (ODFs) are calculated. The φ_1, Φ and φ_2 angles are the conventional Euler angles.

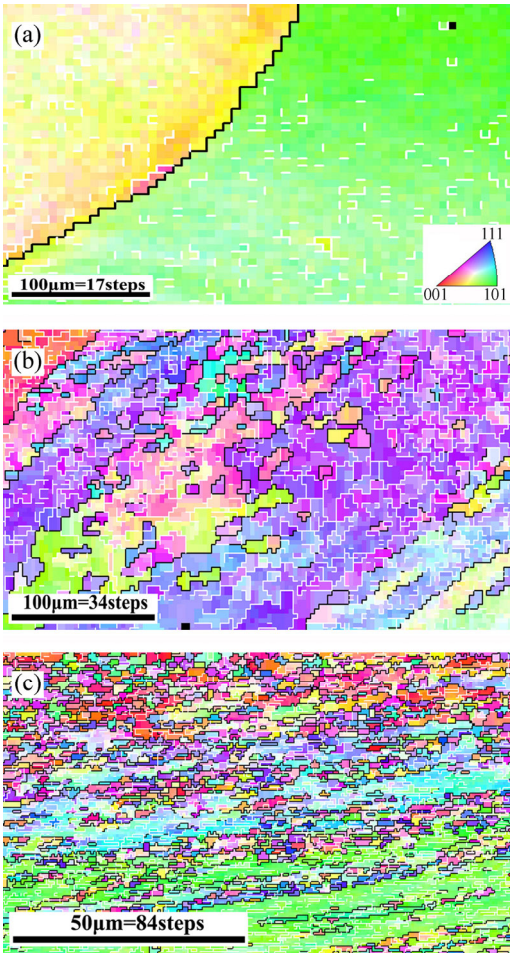

Fig. 4 OIM images for high purity aluminum under initial unpressed condition (a) and first pass (b), and fifth pass (c)

Figures 5(a)−(c) show the ODF maps of the initial metal and the sample after the one press and the sample after five presses, respectively. For convenience, the φ_2=0° in the ODF is used to illustrate the texture components (Fig. 5(d)). The orientation line analysis of α-fibers is selected at the peaked angle of (0°≤φ_1≤90°, φ_2=0°, Φ=45°). It can be seen that the initial texture has completely vanished and the significant texture changes occur after five passes, and the α-fiber of the five passes is peaked at near {011}<011> texture. Thus, after five passes, the initial texture is replaced by new components close to (80°, 35°, 0°), (40°, 75°, 45°) and (0°, 85°, 45°) (Fig. 5(c)), and the overall intensity of microtexture is decreasing with increasing the number of passes.

3.4 Characteristics of grain boundaries in samples

Correlated misorientations distribution function (MDF) can be used to resolve the orientation relationship between grains. Figures 6(a)−(c) show the axis preference of misorientations of the initial metal and the sample after the one press and the sample after five presses, respectively. The degree of axis preference was characterized as a multiple of random distribution (MRD), and higher numbers indicate stronger preferences. It can be seen that some misorientations peaks in the initial metal have disappeared in the following passes, and the strong misorientations distribution peak 90° [001] exists from initial state to fifth pass, and the maximal intensity of MRD gradually decreased from 120.5 to 38.0 after five passes. Thus, the grain boundary misorientations distributions gradually change by the severe shear deformation, and the misorientations distributions become random with increasing the number of passes.

The grains boundary misorientations measured with EBSD are shown in Fig. 7. A high fractions of low-angle boundaries is present in the initial materials for the bulk grain size (Fig. 7(a)). The fraction of the HABs

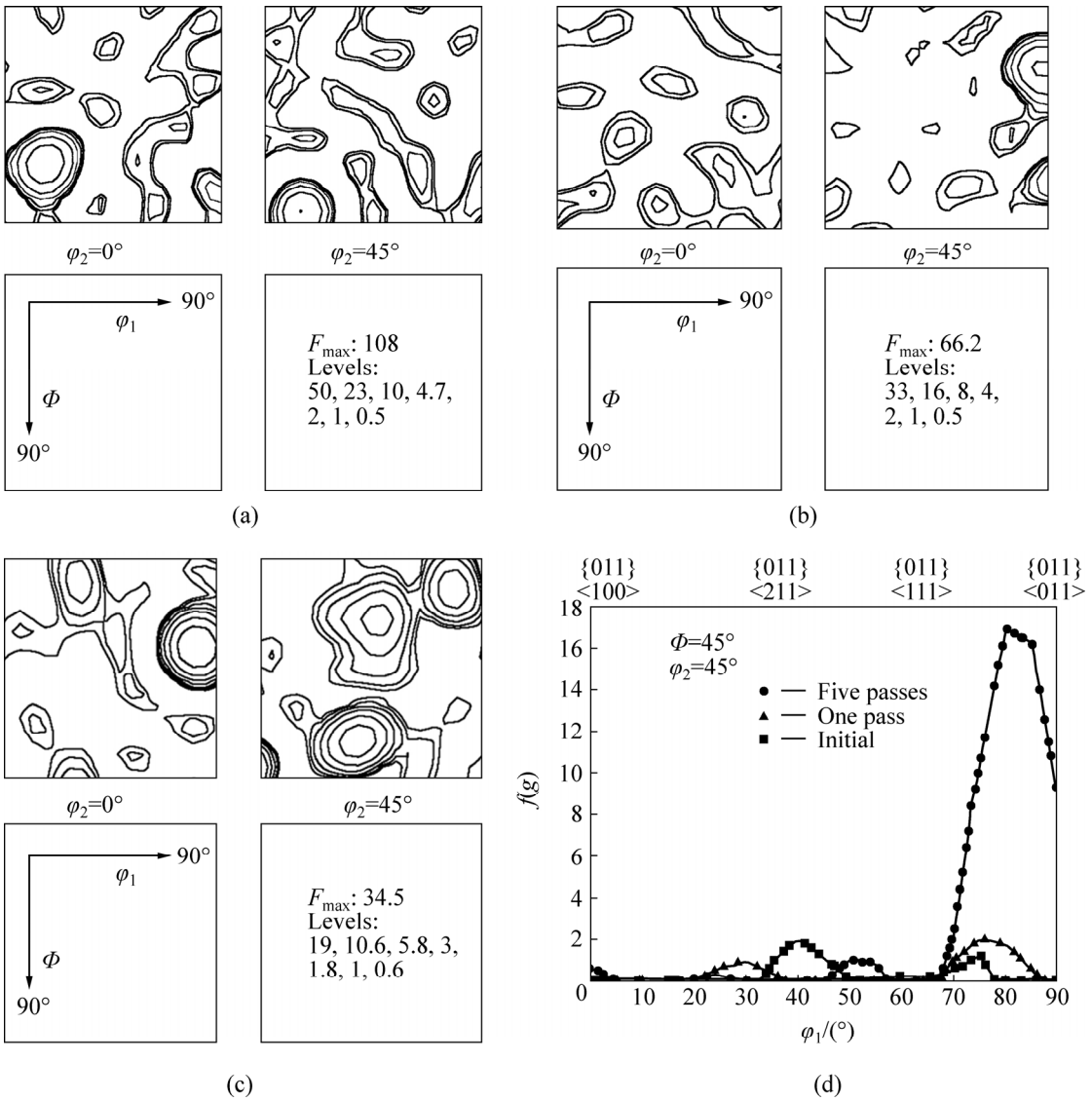

Fig. 5 ODF sections at φ_2=0° and φ_2=45° for sample: (a) At initial state; (b) After one pass; (c) After five passes; (d) Corresponding maximum intensity along α-fiber

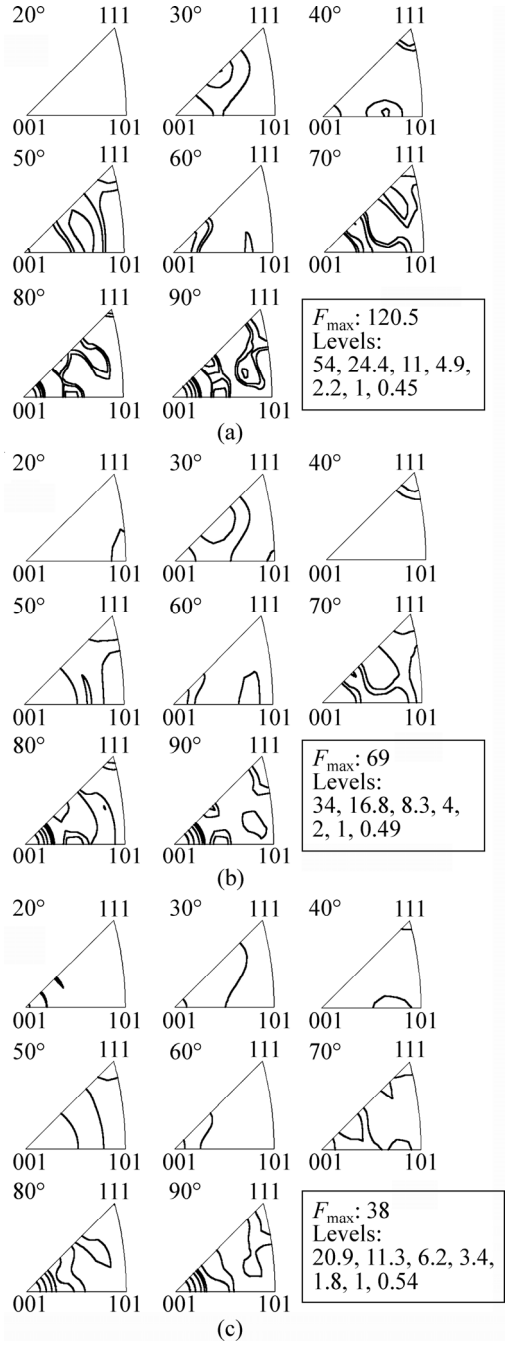

Fig. 6 MDF of grain boundaries for sample: (a) At initial state; (b) After one pass; (c) After five passes

increases as the ECAP proceeds. The HABs fractions are about 0.21 and 0.46 after one pass and five passes (Figs. 7(b) and (c)), respectively. LIU and HANSEN [21] classified deformation-induced boundaries into incidental dislocation boundaries (IDBs) and geometrical necessary boundaries (GNBs). The cellblocks and the ordinary dislocation cells structures were bounded by GNBs and IDBs, respectively. The misorientation across GNBs should be much larger than across IDBs and rise faster with increasing strain [21]. Boundaries resulting from grain subdivision should be GNBs. It suggests that those grain boundaries are GNBs with aim of accommodating the imposed shear strain. Therefore, low-angle misorientations evolve toward large angles with straining, which may be caused by the rotation of subgrains during pressing. The nearly random distribution of orientations and the progressive increase in misorientations between deformation subgrains during plastic deformation are typical features of cDRX [22−24].

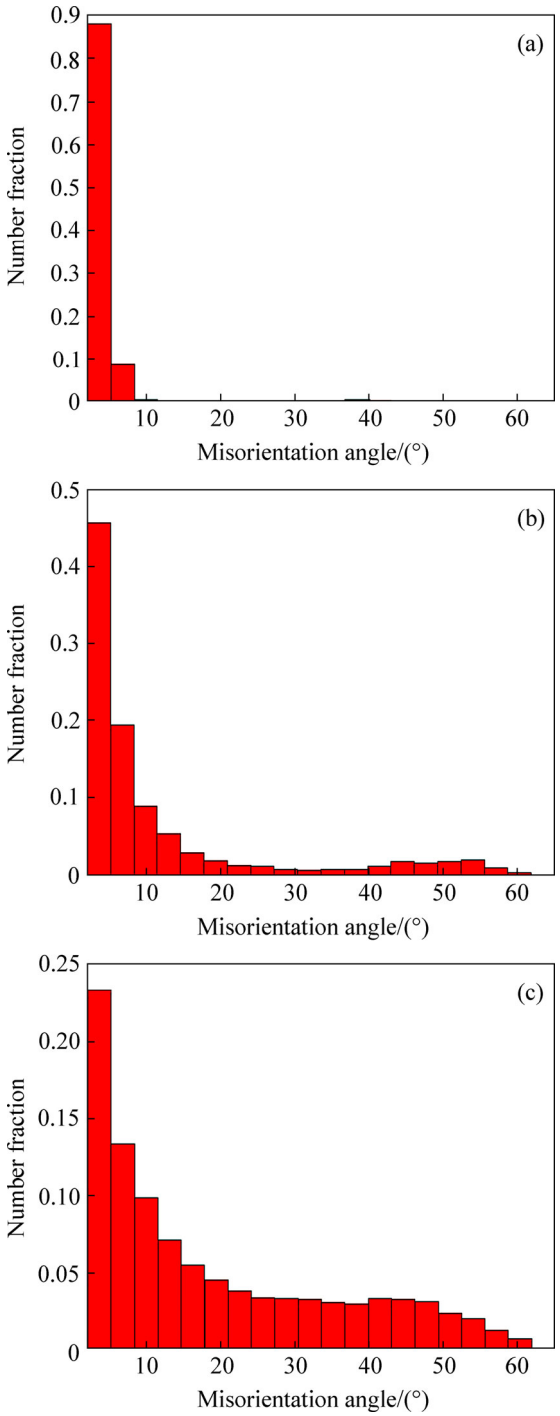

Fig. 7 Misorientation distributions for boundaries in sample: (a) At initial state; (b) After one pass; (c) After five passes

3.5 Mechanism of microstructure evolution

Two means are used to produce a fine-grain microstructure [25−27]. One is discontinuous

recrystallization (dRX), which involves the nucleation and growth of strain-free grains. The driving for dRX is stored dislocations acting on high mobility boundaries; it may occur during hot deformation (i.e. dynamic recrystallization) or during heat treatment following cold or hot deformation (i.e. classical static recrystallization). The misorientations across the new grain boundaries are usually high. SALEM et al [15] found that the dRX occurred in the high-purity aluminum most likely following, not during severe plastic deformation. The other method to produce fine grain microstructure is continuous recrystallization (cRX). A microstructure containing high-angle grain boundaries (HAGBs) may evolve continuously during large plastic deformation under cold- or warm-working conditions, producing an ultra-fine-grained material. We found that the microtexture and grain boundary misorientations in the high-purity aluminum evolve continuously from the initial state to the fifth pass during ECAP process with the assistant of the mechanical forces (Figs. 5−6), and the grain boundaries among the ultrafine grains in the high-purity aluminum are GNBs with high-angles (Fig. 7). Therefore, it is suggested that the mechanical deformation assistants the grain boundaries' evolution and the continuous dynamic recrystallization (cDRX) mechanism dominates the microstructure evolution in the present work.

Figure 8 illustrates the microstructure evolution in the high purity aluminum processed by ECAP: 1) A large number of elongated cell structures are formed by cold deformation; 2) Those cell structures are easily transformed to the subgrains owing to the dynamic annihilation of dislocation during deformation processes; 3) The rotation of a subgrains to different preferred crystal orientations with strain increasing (Fig. 5(c)), a process which creates the high angle boundaries (Fig. 7(c)), and uniform equiaxed grains of diameters about 0.9 μm with random orientation distribution are formed.

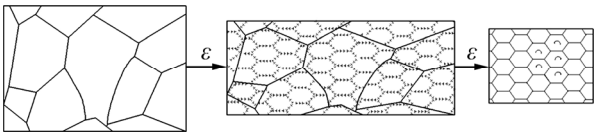

Fig. 8 Schematic of grain refinement during ECAP process

4 Conclusions

1) Pressing up to the five the pass, the microstructure of high purity aluminum evolves from elongated cell structures to a number of ultrafine equiaxed grains with diameters about 0.9 μm and low dislocation density.

2) The grain boundaries of ultrafine equiaxed grains are GNBs with high fraction of high-angle boundaries. The orientations distribution of grains in the specimens evolve toward random orientation distribution; however, the microtextures (80°, 35°, 0°), (40°, 75°, 45°) and (0°, 85°, 45°) are peaked in the sample after five passes.

3) The grain refinement of the high purity aluminum proceeded by ECAP can be elucidated by cDRX.

References

[1] ESTRIN Y, MURASHKIN M, VALIEV R. Ultrafine-grained aluminum alloys: Processes, structural features and properties [C]// LUMLEY R. Fundamentals of Aluminum Metallurgy: Production, Processing and Applications. Cambridge: Woodhead Publ Ltd, 2011: 468−503.

[2] KUMAR S R, GUDIMETLA K, VENKATACHALAM P, RAVISANKAR B, JAYASANKAR K. Microstructural and mechanical properties of Al 7075 alloy processed by equal channel angular pressing [J]. Materials Science and Engineering A, 2012, 533: 50−54.

[3] QIAN T, MARX M, SCHULER K, HOCKAUF M, VEHOFF H. Plastic deformation mechanism of ultra-fine-grained AA6063 processed by equal-channel angular pressing [J]. Acta Materialia, 2010, 58(6): 2112−2123.

[4] ZHAO Jun, WANG Zhen-hua, SUN Shu-hua, ZHAO De-li, REN Li-guo, FU Wan-tang. A new method of characterizing equivalent strain for equal channel angular processing [J]. Journal of Central South University of Technology, 2009, 16(3): 349−353.

[5] VEVEÇKA A, CABIBBO M, LANGDON T G. A characterization of microstructure and microhardness on longitudinal planes of an Al-Mg-Si alloy processed by ECAP [J]. Materials Characterization, 2013, 84: 126−133.

[6] ZHOU Yin-yu, LIU Fang, DU Fei-peng. Finite element analysis for effect of die parameters on deformation of equal channel angular pressing of pure titanium [J]. Journal of Materials and Metallurgy, 2014, 13(1): 66−70. (in Chinese)

[7] HEBESBERGER T, STUWE H P, VORHAUER A, WETSCHER F, PIPPAN R. Structure of Cu deformed by high pressure torsion [J]. Acta Materialia, 2005, 53(2): 393−402.

[8] AAL M I A E, KIM H S. Wear properties of high pressure torsion processed ultrafine grained Al-7%Si alloy [J]. Materials and Design, 2014, 53: 373−382.

[9] ZHANG Zi-zhao, XU Xiao-chang, HU Nan, QU Xiao, CHEN Zhen-xiang. Re-ageing behavior of Al-Cu alloy after re-dissolution of precipitated phases caused by severe plastic deformation [J]. Journal of Central South University, 2010, 41(5): 1782−1790. (in Chinese)

[10] WANG Bing-feng, LIU Zhao-lin, LI Juan. Microstructure evolution in AISI201 austenitic stainless steel during the first compression cycle of multi-axial compression [J]. Materials Science and Engineering A, 2013, 568: 20−24.

[11] SU Li-hong, LU Cheng, LI Hui-jun, DENG Guan-yu, TIEU K. Investigation of ultrafine grained AA1050 fabricated by accumulative roll bonding [J]. Materials Science and Engineering A, 2014, 614: 148−155.

[12] ROY S, NATARAJ B R, SUWAS S, KUMAR S, CHATTOPADHYAY K. Accumulative roll bonding of aluminum alloys 2219/5086 laminates: Microstructural evolution and tensile properties [J]. Materials and Design, 2012, 36: 529−539.

[13] TALACHI A K, EIZADJOU M, MANESH H D, JANGHORBAN K. Wear characteristics of severely deformed aluminum sheets by accumulative roll bonding (ARB) process [J]. Materials

Characterization, 2011, 62(1): 12−21.

[14] IWAHASHI Y, HORITA Z, NEMOTO M, LANGDON T G. An investigation of microstructural evolution during equal-channel angular pressing [J]. Acta Materialia, 1997, 45(11): 4733−4741.

[15] SALEM A A, LANGDON T G, MCNELLEY T R, KALIDINDI S R, SEMIATIN S L. Strain-path effects on the evolution of microstructure and texture during the severe-plastic deformation of aluminum [J]. Metallurgical and Materials Transaction A, 2006, 37(9): 2879−2891.

[16] QU Shen, AN Xiang-hai, YANG Hua-jie, HUANG Chong-xiang, YANG Gang, ZANG Qi-shan, WANG Zhong-guang, WU Shi-ding, ZHANG Zhe-feng. Microstructural evolution and mechanical properties of Cu-Al alloys subjected to equal channel angular pressing [J]. Acta Materialia, 2009, 57(5): 1586−1601.

[17] XU W, WU X, CALIN M, STOICA M, ECKERT J, XIA K. Formation of an ultrafine-grained structure during equal-channel angular pressing of a β-titanium alloy with low phase stability [J]. Scripta Materialia, 2009, 60(11): 1012−1015.

[18] LIN Zheng-jie, WANG Li-qiang, XUE Xiao-bing, LU Wei-jie, QIN Ji-ning, ZhANG Di. Microstructure evolution and mechanical properties of a Ti-35Nb-3Zr-2Ta biomedical alloy processed by equal channel angular pressing (ECAP) [J]. Materials Science and Engineering C, 2013, 33(8): 4551−4561.

[19] CHANG J Y, YOON J S, KIM G H. Development of submicron sized grain during cyclic equal channel angular pressing [J]. Scripta Materialia, 2001, 45(3): 347−354.

[20] IWAHASHI Y, WANG Jing-tao, HORITA Z J, NEMOTO M, LANGDON T G. Principle of equal-channel angular pressing for the processing of ultra-fine grained materials [J]. Scripta Materialia, 1996, 35(2): 143−146.

[21] LIU Qing, HANSEN N. Geometrically necessary boundaries and incidental dislocation boundaries formed during cold deformation [J]. Scripta Metallurgica et Materialia, 1995, 32(8): 1289−1295.

[22] DUDOVA N, BELYAKOV A, SAKAI T, KAIBYSHEV R. Dynamic recrystallization mechanisms operating in a Ni-20%Cr alloy under hot-to-warm working [J]. Acta Materialia, 2010, 58(10): 3624−3632.

[23] DOHERTY R D, HUGHES D A, HUMPHREYS F J, JONAS J J, JUUL JENSEN D, KASSNER M E, KING W E, MCNELLEY T R, MCQUEEN H J, ROLLETT A D. Current issues in recrystallization: A review [J]. Materials Science and Engineering A, 1997, 238(2): 219−274.

[24] BELYAKOV A, GAO W, MIURA H, SAKAI T. Strain-induced grain evolution in polycrystalline copper during warm deformation [J]. Metallurgical and Materials Transactions A, 1998, 25(12): 2957−2965.

[25] HUMPHREYS F J, PRANGNELL P B, PRIESTNER R. Fine-grained alloys by thermomechanical processing [J]. Current Opinion in Solid State and Materials Science, 2001, 5(1): 15−21.

[26] CHENG Wei-li, LI Jia-wei, QUE Zhong-ping, ZHANG Jin-shan, XU Chun-xiang, LIANG Wei, YOU B S, PARK S S. Microstructure, texture and tensile properties of Mg-10Sn alloys extruded in different conditions [J]. Journal of Central South University, 2013, 20(7): 1786−1791.

[27] GOURDET S, MONTHEILLET F. An experimental study of the recrystallization mechanism during hot deformation of aluminum [J]. Materials Science and Engineering A, 2000, 283(1/2): 274−288.

(Edited by DENG Lü-xiang)